

Supplementary material for: Optimal design for the Josephson mixer

J.-D. Pilllet,^{1,2} E. Flurin,¹ F. Mallet,^{1, a)} and B. Huard¹

¹⁾*Laboratoire Pierre Aigrain, Ecole Normale Supérieure-PSL Research University, CNRS, Université Pierre et Marie Curie-Sorbonne Universités, Université Paris Diderot-Sorbonne Paris Cité, 24 rue Lhomond, 75231 Paris Cedex 05, France*

²⁾*Collège de France, 11 place Marcelin Berthelot, 75005 Paris, France*

^{a)}corresponding author: francois.mallet@lpa.ens.fr

I. EXTRACTION OF THE CIRCUIT'S ELECTRICAL PARAMETERS

The electrical parameters given in the main text of the letter were obtained by numerical simulations as well as fit of the measured quality factor as a function of the resonant frequency (insets of Fig. 3 (a)). Each of the resonators of our device is modeled by the circuit shown in Fig. 1 constituted by a 50Ω transmission line and an LC resonator. For a (resp. b), the impedance $Z^{a(b)}$ of the LC resonator as seen from the transmission line is given by:

$$Z^{a(b)} = \frac{j \left(L_{ex}^{a(b)} + L_J/2 \right) \omega \times \left(L_{stray}^{a(b)} - 1 / \left(C_{res}^{a(b)} \omega^2 \right) \right)}{L_{ex}^{a(b)} + L_J/2 + L_{stray}^{a(b)} - 1 / \left(C_{res}^{a(b)} \omega^2 \right)},$$

whose pole gives the resonant frequency $\omega_{a(b)} = \frac{1}{\sqrt{\left(L_{ex}^{a(b)} + L_J/2 + L_{stray}^{a(b)} \right) \times C_{res}^{a(b)}}}$. From $Z^{a(b)}$, the reflection coefficient of a signal sent in the transmission line and reflected on the resonator can be expressed as

$$r^{a(b)} = \frac{Z - Z_c}{Z + Z_c},$$

where Z_c is the characteristic impedance of the transmission line and equal to 50Ω . Near $\omega \approx \omega_{a(b)}$, this expression may be written

$$r^{a(b)} = \frac{\omega^2 - \omega_{a(b)}^2 - j\omega\omega_{a(b)}/Q_{a(b)}}{\omega^2 - \omega_{a(b)}^2 + j\omega\omega_{a(b)}/Q_{a(b)}},$$

where $Q_{a(b)}$ is the quality factor. The latter depends on the resonant frequency through the equation

$$Q_{a(b)} = \frac{Z_c C_{res}^{a(b)} \omega_{a(b)}}{\left(1 - L_{stray}^{a(b)} C_{res}^{a(b)} \omega_{a(b)} \right)}. \quad (1)$$

Thanks to parameters obtained from the full 3D simulations of the whole device (see main text), we used Eq. 1 to fit experimental data of the insets of Fig. 3 (a) and deduce the stray inductances of the capacitors of resonators a and b . Our best fits are obtained for $L_{res}^a = 75$ pH and $L_{res}^b = 51$ pH.

II. CALIBRATION USING THE DEPENDENCE OF RESONANT FREQUENCY ON INPUT POWER

In the main text of the letter, we have evaluated the efficiency of the Josephson amplifier thanks to a calibration of the input and output lines of our setup. We obtain it taking

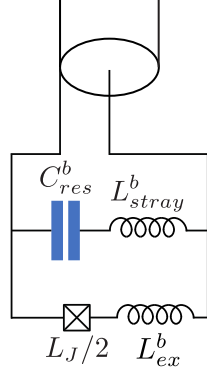


FIG. 1. Electrical model describing resonator b of the Josephson ring including parasitic geometric inductances L_{ex}^b and L_{stray}^b .

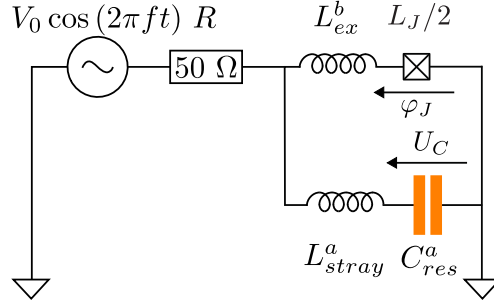


FIG. 2. Simulated circuit for the calibration of our setup.

advantage of the shift of the resonant frequency while sweeping P_{in} . For this, we have measured the resonant frequency of mode a as a function of the power delivered by our vector network analyzer (VNA) and have compared our measurements to a full numerical simulation of the device. This way, we can deduce the corresponding actual P_{in} at the level of the device for a given power injected at the input of our setup. The non-linearity of our device is so high that we have to take into account higher orders terms, we thus don't only consider the lowest order Kerr term $(a^\dagger a)^2$ coming from the development in series of $\cos(\varphi_J)$ as it is usually done, but we take into account terms to all order by keeping the full cosine.

The circuit that we simulated is shown in Fig. 2, a 50Ω resistor models the dissipation due to losses of the resonator into the 50Ω transmission line, and the microwave source of the VNA is modeled by an ac voltage source supplying a power $P_{in} = V_0^2/4R$. Applying Kirchoff's law, one can show that it obeys the following set of coupled equations:

$$\frac{U'_C(t)}{\varphi_0} + \frac{\varphi'_J(t)}{RC_{res}^a} + \frac{I_c}{\varphi_0 C_{res}^a} \sin(\varphi_J(t)) + \frac{L_{ex}^a I_c}{\varphi_0 RC_{res}^a} \varphi'_J(t) \cos(\varphi_J(t)) = \frac{V_0 \cos(2\pi ft)}{\varphi_0 RC_{res}^a} \quad (2)$$

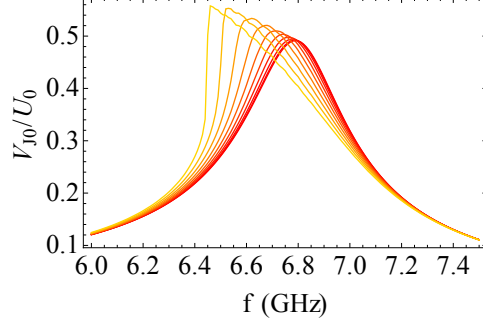


FIG. 3. Calculated response of the circuit of Fig. 2 using the electrical parameters of section I and for $\varphi_{ext} = 0.645 \times \pi/2$. The amplitude V_{J0} of the voltage across the Josephson junction (normalized by the amplitude of the excitation V_0) is plotted as a function of the frequency f of the excitation for increasing V_0 from red to yellow. At low V_0 , it appears as a Lorentzian function centered on the resonant frequency of resonator a . The latter shifts toward lower frequency for increasing V_0 , then the Lorentzian function becomes asymmetric and bends in direction of the lower frequency until the circuit becomes bistable and a discontinuity appears on the left side of the Lorentzian.

$$L_{stray}^a C_{res}^a U_C''(t) + U_C(t) = \varphi_0 \varphi_J'(t) + L_{ex}^a I_c \varphi_J'(t) \cos(\varphi_J(t)). \quad (3)$$

Here U_C the voltage across the capacitor, φ_0 is the flux quantum, φ_J is the phase across the Josephson junction and I_c is the critical current of the junction with

$$I_c = \frac{2\varphi_0}{L_J} \sin(\varphi_{ext}), \quad (4)$$

where $\varphi_{ext} = \Phi/4\varphi_0$, Φ being the flux threading the loop of the Josephson ring.

We numerically solved the set of Eq. 2 and 3 as a function of the time t with the initial condition $U_C(0) = 0$, $\varphi_J(0) = 0$, $U_C'(0) = 0$ and using the electrical parameters of section I. For a given amplitude V_0 , frequency of excitation f and after a transient regime of a few nanoseconds, the voltage across the junction $V_J(t) = \varphi_0 \varphi_J'(t)$ behaves as a periodic function whose amplitude V_{J0} is maximal when f matches the resonant frequency of the circuit. Fig. 3 shows the responses of the circuit for increasing V_0 and it is clear that the resonant frequency moves toward lower frequency. At high values of V_0 , we observe as expected that the resonator becomes bistable which induces a discontinuity of the amplitude when sweeping the frequency. Comparing the results of this simulation with our experimental measurements as we did in Fig. 4 a of the main text, we were able to deduce an attenuation in the input line of approximately 86.5 dB.

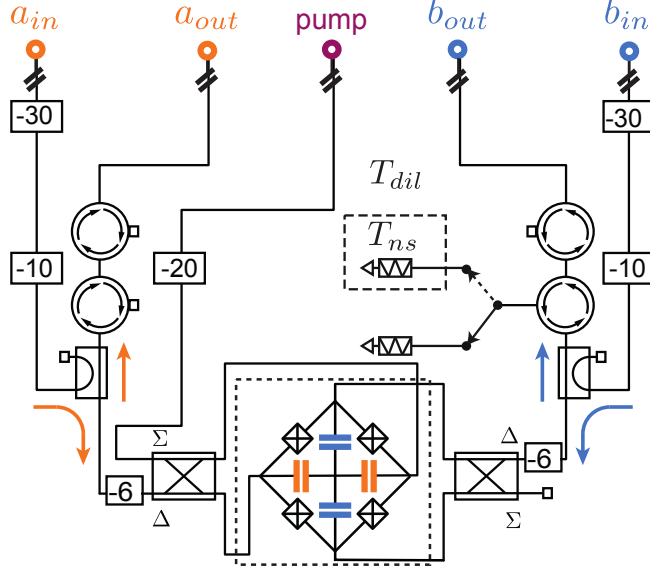


FIG. 4. Schematic of the experimental setup. Normal Modes are addressed in reflection through two 180° hybrid couplers, all input lines being filtered and attenuated (partially shown). Output signals are separated from input signals by a directional coupler and amplified by a low noise HEMT amplifier at the 4K stage (following room temperature amplifiers chain not shown). For the added noise calibration, a switch connects input of port b to either vacuum noise from a 50Ω load at T_{dil} , either thermal noise of a thermally isolated 50Ω load of variable temperature T_{ns} .

III. NOISE CALIBRATION WITH THERMAL NOISE

On top of the calibration of the added noise presented in the main text, the amplifier added noise has also been evaluated by connecting port b to a 50Ω load with a tunable temperature T_{ns} , thermally isolated from the rest of the circuit. The output noise density S_{ON} (resp. S_{OFF}) is recorded while the Josephson amplifier is turned on (resp. off). The frequency of the pump is 12.16 GHz and the power is chosen such that the gain reaches approximately 32 dB when the amplifier is on.

The measurement setup is sketched in Fig. 5. Two beamsplitters with $1/4$ transmission represents the 6 dB attenuator and another one, at the input of the amplifier, with transmission η models the efficiency of the device.

When the amplifier is off (*i.e.* pump is off), the noise measured by the spectrum analyzer is given by

$$S_{OFF} = S_{LNA} + G_{LNA} \left[\frac{3}{4} S_{dil}^{out} + \frac{1}{4} \left(\frac{\eta}{4} S_{ns} + \left(1 - \frac{\eta}{4} \right) S_{dil}^{in} \right) \right], \quad (5)$$

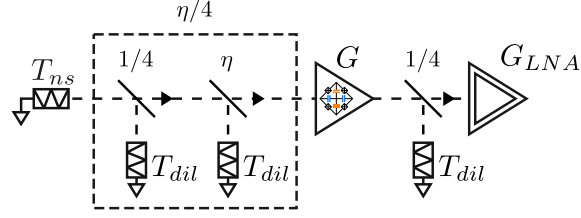


FIG. 5. Schematic of the measurements for the noise calibration of our device using a 50Ω source of thermal noise. The 6 dB attenuator plugged at the input and output of the Josephson amplifier are modeled as beamsplitters with $1/4$ transmission while the internal losses of the device are modeled with a η transmission beamsplitter. The $1/4$ and η transmission beamsplitters combined are equivalent to a single beamsplitter with $\eta/4$ transmission.

with S_{LNA} the added noise of the HEMT amplifier at 4 K, G_{LNA} its gain, S_{dil}^{out} (resp. S_{dil}^{in}) the noise introduced by the 6 dB attenuator at the output (resp. input) of the Josephson amplifier at the fridge temperature, and S_{ns} is the noise emitted by 50Ω load with variable temperature T_{ns} . At the base temperature of our fridge we have $S_{dil}^{out} = S_{dil}^{in} = S_{dil}$ with $S_{dil} = 1/2 \coth[hf_b/2k_B T]$ ($S_{dil} \approx 1/2$ since the temperature in the dilution fridge $T_{dil} \ll hf_b/k_B = 260$ mK). Similarly, when the amplifier is on, the noise can be expressed as

$$S_{ON} = S_{LNA} + G_{LNA} \left[\frac{3}{4} S_{dil}^{out} + \frac{1}{4} G \left(\frac{\eta}{4} S_{ns} + \left(1 - \frac{\eta}{4}\right) S_{dil}^{in} \right) + \frac{1}{4} (G - 1) S_{dil} \right]. \quad (6)$$

The last term is due to the amplification of the zero point fluctuation of the a resonator, G being the gain of the Josephson amplifier.

The difference between ON (Eq. 6) and OFF (Eq. 5) power spectral densities is given by

$$\frac{S_{ON} - S_{OFF}}{hf_a G} = \frac{\eta G_{LNA}}{4} \left[\frac{S_{ns}}{4} + \frac{3}{4} S_{dil} + \frac{2 - \eta}{\eta} S_{dil} \right]. \quad (7)$$

The first term in Eq. 7 is the amplified signal coming from the noise source, the second one is the total added noise introduced by the -6 dB attenuator, and the third one is the added noise of the Josephson amplifier.

For a perfect device with $\eta = 1$, the added noise of the Josephson amplifier is half a photon, while for a realistic amplifier there will be an extra noise equal to $(1 - \eta)/\eta$ photons. By fitting the measured spectral density of Fig. 6 as a function of T_{ns} with Eq. 7, we extract $G_{LNA} \approx 62.3$ dB and an efficiency $\eta \approx 0.62$ which corresponds to an extra noise of 0.6 photon, consistent with the other calibration on resonator a .

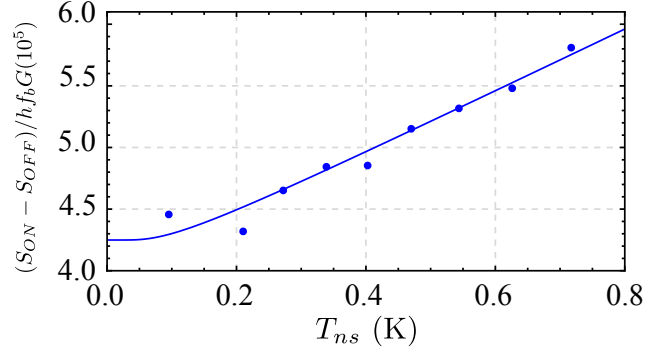


FIG. 6. Difference between measured spectral densities out of resonator b , its input being connected to the noise source, as a function of T_{ns} when the pump is turned on (S_{ON}) and when the pump is turned off (S_{OFF}). The experimental data, appearing as blue dots, are normalized by the energy of a quantum in resonator b and the gain G of the Josephson amplifier set to be approximately 32 dB. Continuous line: fit of these data using Eq. 7.